Supporting information

Single-Atom Pd_1/graphene Catalyst Achieved by Atomic Layer Deposition: Remarkable Performance in Selective Hydrogenation of 1,3-Butadiene

Huan Yan,[†] Hao Cheng,[†] Hong Yi,[†] Yue Lin, Tao Yao, Chunlei Wang, Junjie Li, Shiqiang Wei,* Junling Lu [*]

*To whom correspondence should be addressed. E-mail: junling@ustc.edu.cn and

sqwei@ustc.edu.cn

Experimental section

Figures S1-S17

Tables S1-S5

References

Experimental section

Pristine graphene nanosheet (99.5%, Chengdu Organic Chemicals Co. Ltd., Chinese Academy of Sciences) was first oxidized to graphene oxide according to the procedure described previously.[1] In brief, 0.6 g graphene nanosheet and 0.3 g sodium nitrate was sequentially added into concentrated sulphuric acid (H_2SO_4, 15 ml) and stirred at room temperature for 22 h. Then, 1.8 g potassium permanganate ($KMnO_4$) was added after cooling down the mixture to 0 ℃. The mixture was then sequentially stirred at room temperature and 35 ℃ for 2 h and 3h, respectively. After that, the mixture was heated to 98 ℃ while adding 30 ml H_2O, and kept at this temperature for 30 min. Then it was cooled down to 40 ℃, and another 90 ml of water and 7.5 ml of hydrogen peroxide (H_2O_2, 30%) were added. Next, the precipitate was filtered out and washed using 300 ml of HCl (5 wt%) for three times, then using de-ioned water for another three times until reaching a neutral pH; it was then dried in a vacuum oven at 45 ℃ overnight. The resulted dry material was grinded to obtain graphene oxide powder. Finally, the graphene support was obtained by thermal deoxygenation of graphene oxide powder at different temperatures and time under helium at a flow rate of 50 ml/min.

Pd ALD was carried out on a viscous flow reactor (GEMSTAR-6^{TM} Benchtop ALD, Arradiance) at 150 ^{o}C using palladium hexafluoroacetylacetate ($Pd(hfac)_2$, Sigma Aldrich, 99.9%) and formalin (Aldrich, 37% HCHO and 15% CH_3OH in aqueous solution).[2-3] Ultrahigh purity N_2 (99.999%) was used as carrier gas at a flow rate of 200 ml min^{-1}. The $Pd(hfac)_2$ precursor container was heated to 65 ℃ to get a sufficient vapour pressure. The chamber was heated to 150 ℃ and the manifold was held at 110 ℃ to avoid precursor condensation. The timing sequence was 120, 120, 60, and 120 sec for $Pd(hfac)_2$ exposure, N_2 purge, formalin exposure and N_2 purge, respectively.

Aberration-corrected HAADF-STEM measurements were taken on a JEM-ARM200F instrument (University of Science and Technology of China) at 200 keV. The Pd lodings were determined by ICP-AES. XPS measurements were taken on

a Thermo-VG Scientific Escalab 250 spectrometer equipped with an Al anode (Al Kα = 1486.6 eV). XAFS measurements at Pd *K*-edge (24 350 eV) were performed in transmission mode with the Si(311) monochromator at BL14W1 beamline of the Shanghai Synchrotron Radiation Facility (SSRF), China. The storage ring of SSRF worked at 3.5 GeV with a maximum current of 210 mA.

Selective hydrogenation of 1,3-butadiene was performed in a fixed-bed quartz tube reactor at atmospheric pressure. The feed gas consists of 1.9% 1,3 butadiene, 4.7% H_2 with Ar as balance gas. For the reaction in the presence of propene, the feed gas was adjusted to 1.9% butadiene, 4.7% H_2, 70% propene and Ar as balance gas. The total flow rate was kept at 25 ml/min in both cases. 45 mg of 0.25wt% Pd_1/graphene catalyst was used, while the amount of other catalysts was adjusted to keep the same Pd content. All catalysts were diluted with 1 g of 60-80 mesh quartz chips. Prior to the reaction test, all catalysts were first calcined in 10% O_2 in Ar then reduced in 10% H_2 in Ar at 150 ℃ for 1h, respectively. The reaction products were analyzed using an online gas chromatography equipped with a FID detector and a capillary column (ValcoPLOT VP-Alumina, 50 m x 0.53 mm) after stabilizing in the feed gas for 2 h.[4] Next, the 1,3-butadiene conversion on all these catalysts was increased by increasing the reaction temperatures.

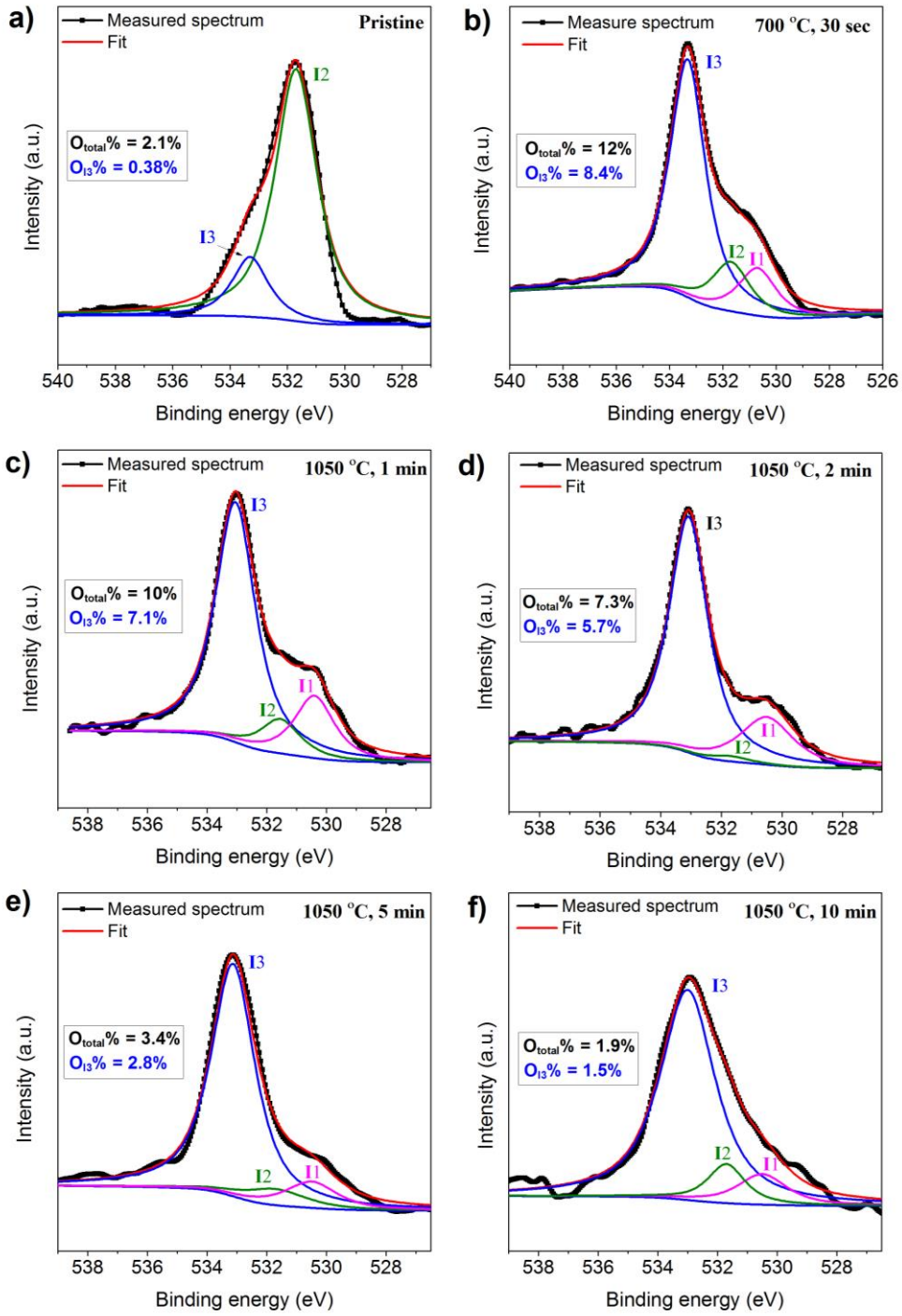

Figure S1. O1s XPS spectra of the pristine graphene nanosheet (a) and the graphene supports obtained by thermal deoxygenation of graphene oxide at 700 ℃ for 30 sec (b), 1050 ℃ for 1 min (c), 1050 ℃ for 2 min (d), 1050 ℃ for 5 min (e), and 1050 ℃ for 10 min (f), respectively. The 3 main peaks at around 531.08, 532.03, and 533.43 eV, deconvoluted from the O1s spectra are assigned to C=O (oxygen doubly bound to aromatic carbon denoted as **I1**), C−O (oxygen singly bonded to aliphatic carbon denoted as **I2**), phenolic oxygen (denoted as **I3**), respectively, according to the literature.[5] Atomic percentages of the total oxygen and I3 oxygen species are indicated.

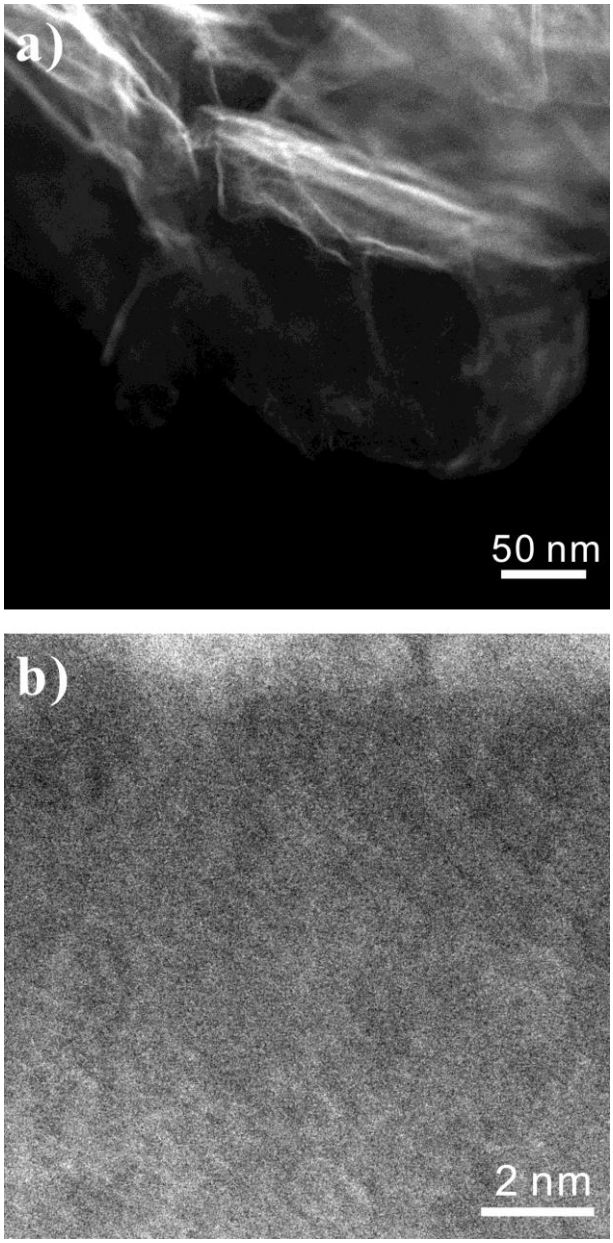

Figure S2. Representative aberration-corrected HAADF-STEM images of the naked graphene at low (a) and high (b) magnifications.

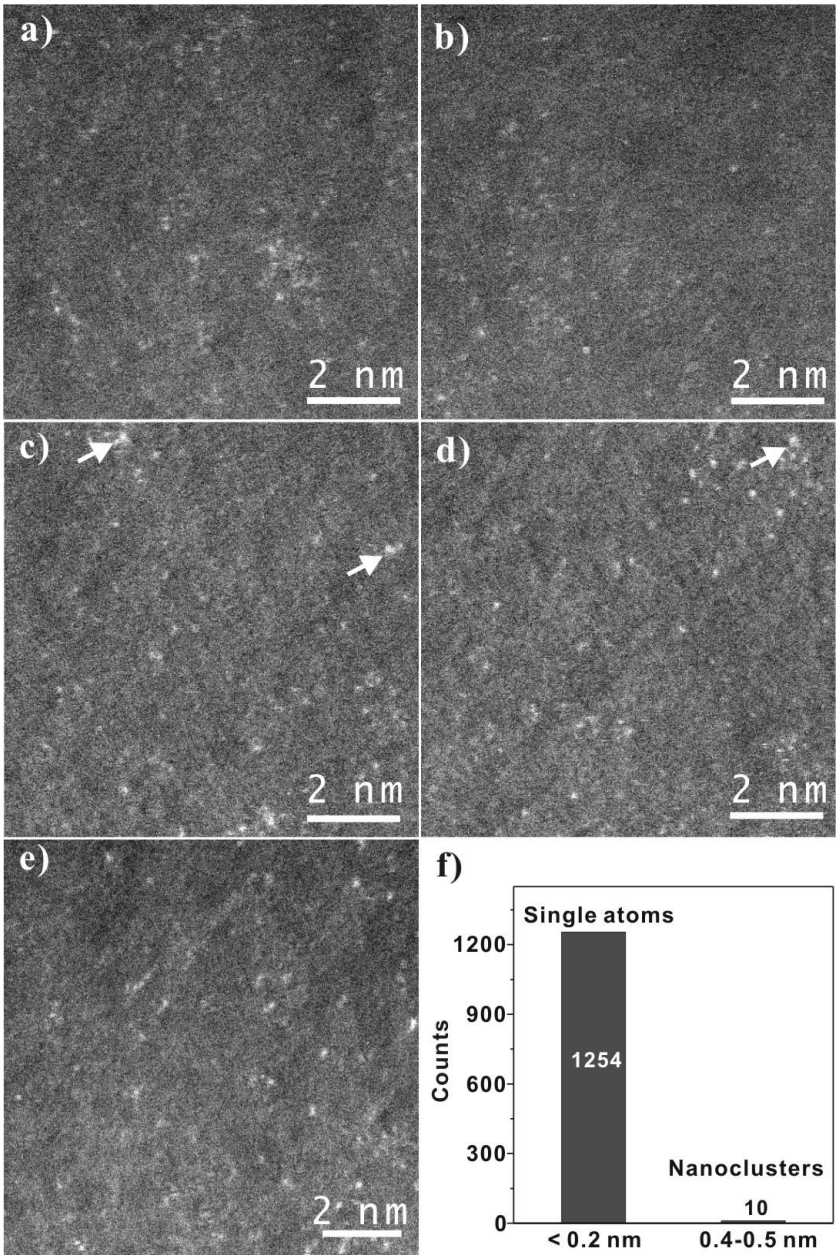

Figure S3. (a-e) Representive aberration-corrected HAADF-STEM images of Pd_1/graphene at other locations. (f) The size distribution on Pd_1/graphene single atom catalyst. The possible Pd nanoclusters are highlighted by the white arrows.

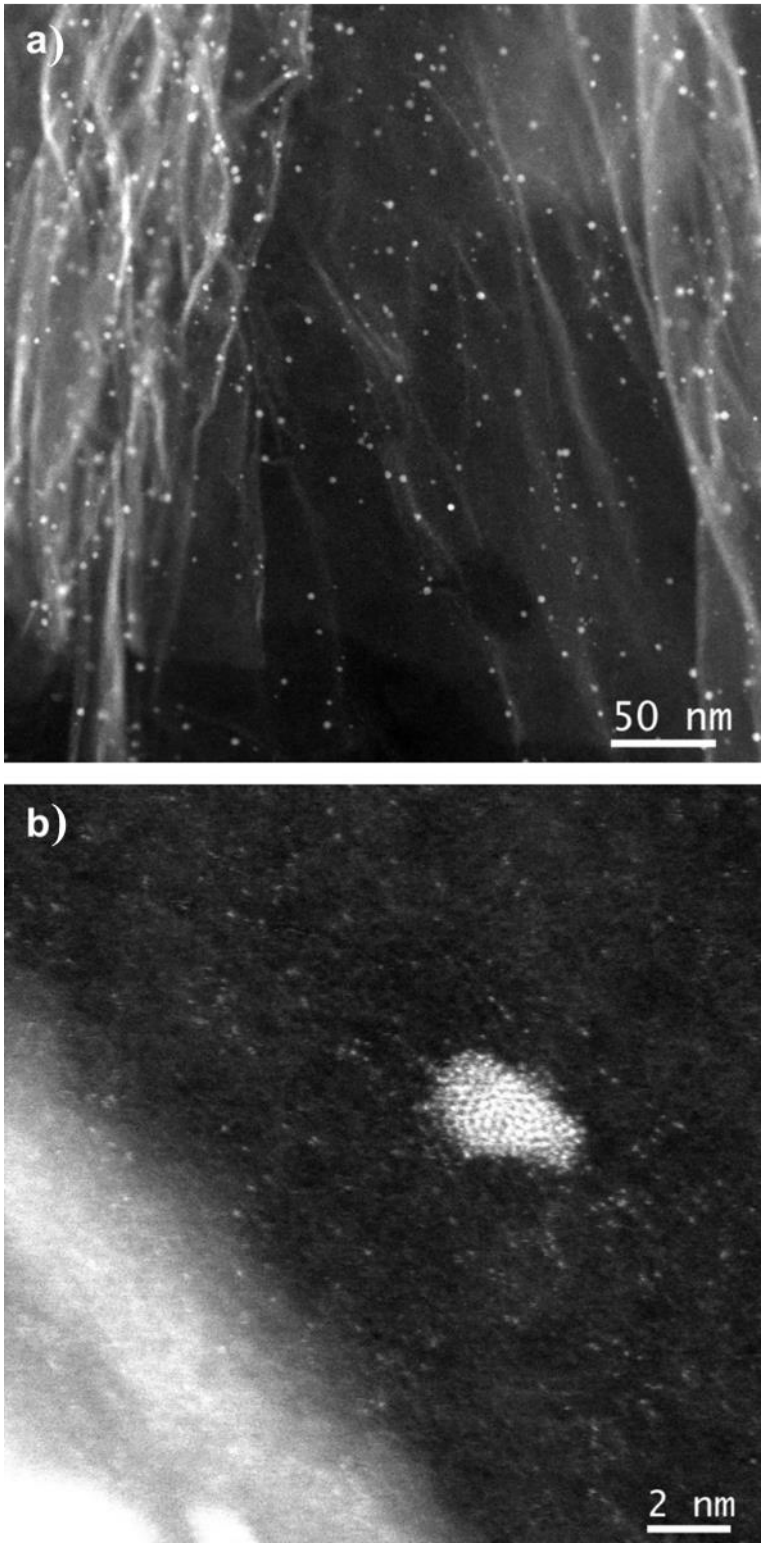

Figure S4. Representative aberration-corrected HAADF-STEM images of the as-prepared Pd-NPs/graphene sample at low (a) and high (b) magnifications. Isolated Pd single atoms and nanoparticles were both observed on this sample. Note: The graphene support in this case was obtained by thermal deoxygenation of graphene oxide at 700 ℃ for 30 sec under helium at a flow rate of 50 ml/min. The average size of Pd nanoparticles was about 3.1 nm.

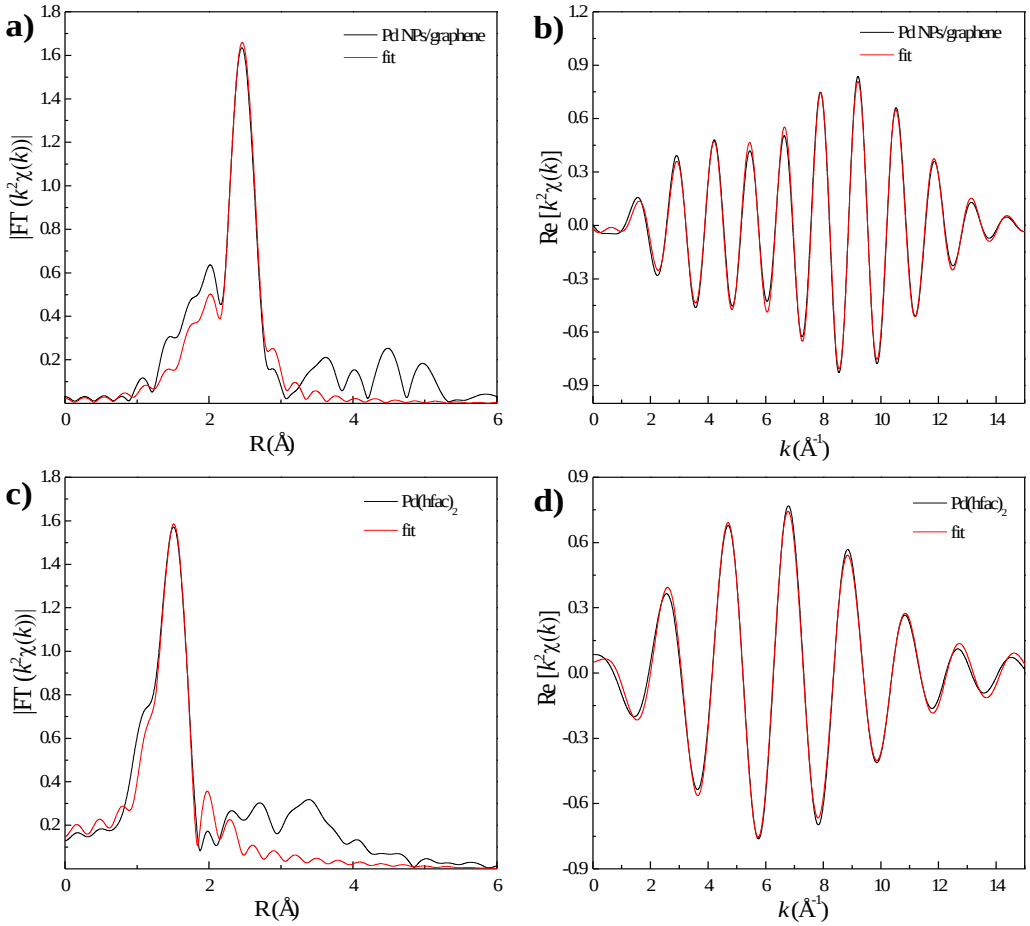

Figure S5. The fitting curve of k^2-weighted EXAFS spectra and $k^2\chi(k)$ oscillations of Pd-NPs/graphene (a-b) and $Pd(hfac)_2$ (c-d), using the ARTEMIS module of IFEFFIT.[6]

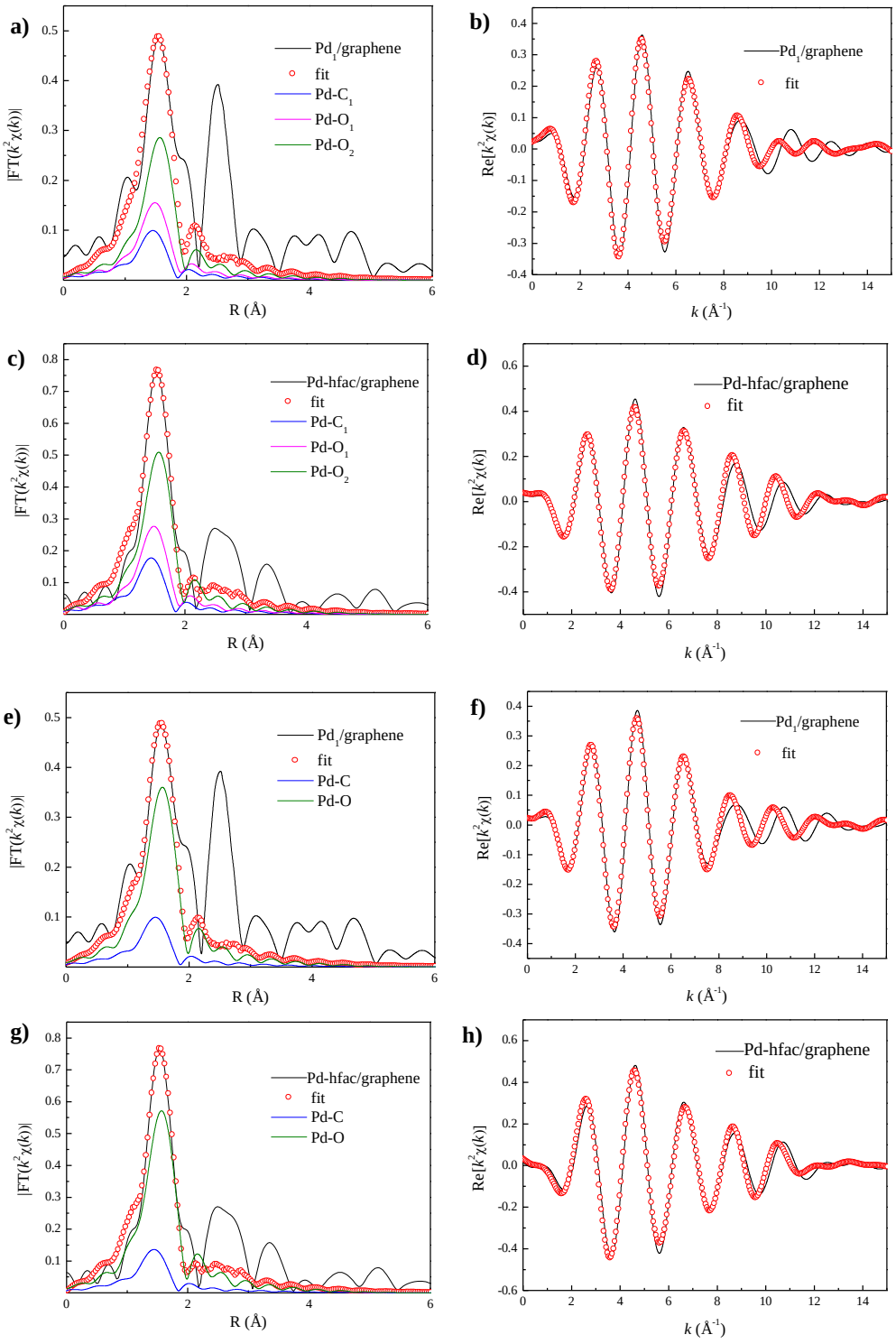

Figure S6. The fitting curve of k^2-weighted EXAFS spectra and $k^2\chi(k)$ oscillations of Pd_1/graphene and Pd-hfac/graphene by considering two Pd-O shells (a-d), and by considering one Pd-O shell (e-h). It can be found that the fitting qualities for two Pd-O shells are the same with that of one Pd-O shells, confirming the rationality of the fitting using two Pd-O shells.

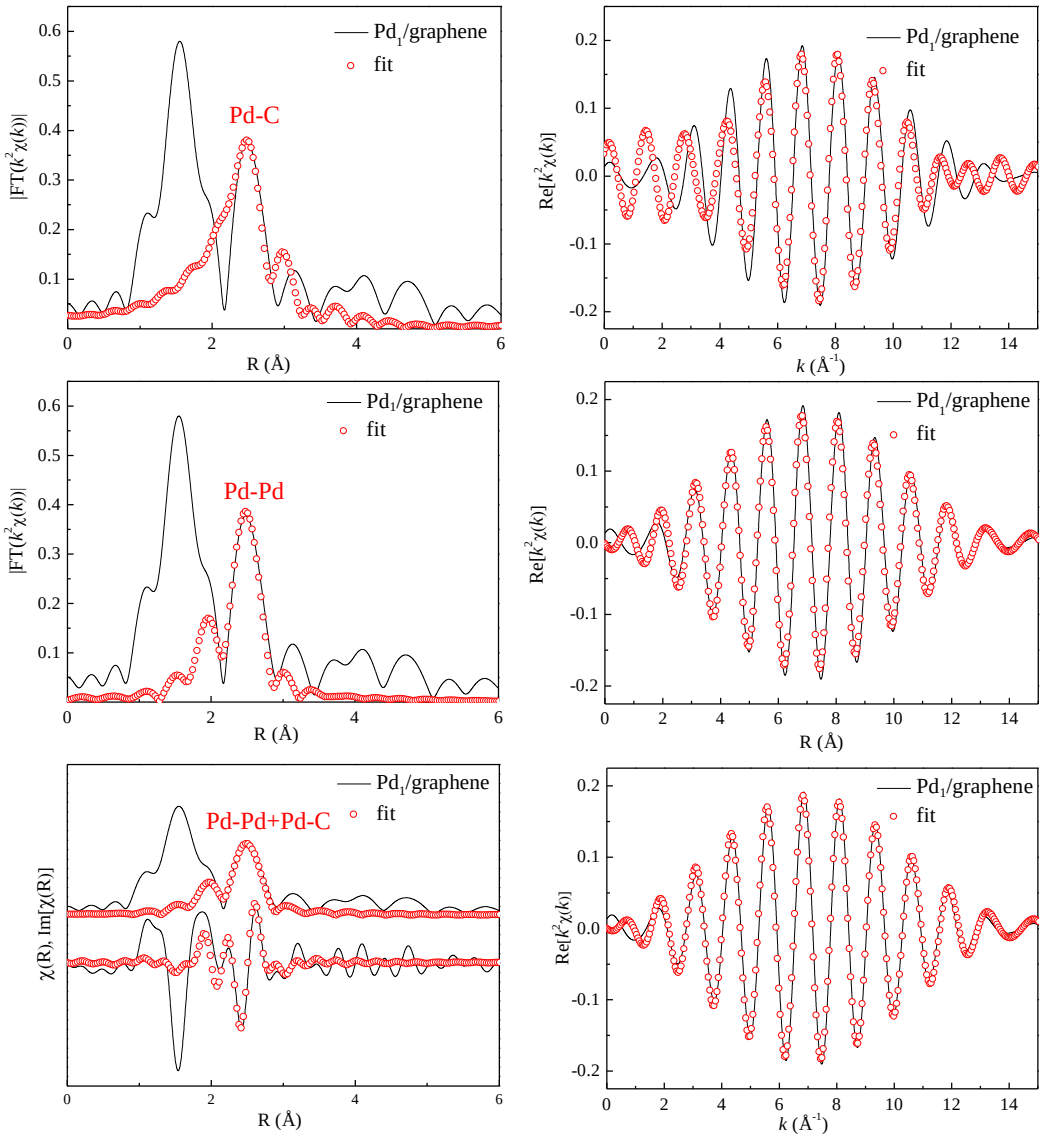

Figure S7. The fitting curve of k^2-weighted EXAFS spectra and $k^2\chi(k)$ oscillations for the second EXAFS FT peak of Pd_1/graphene sample. It can be found that the curve-fitting of the second EXAFS FT peak by including two shells of Pd-C and Pd-Pd can yield a better quality, compared those cases by considering only Pd-C or Pd-Pd shell.

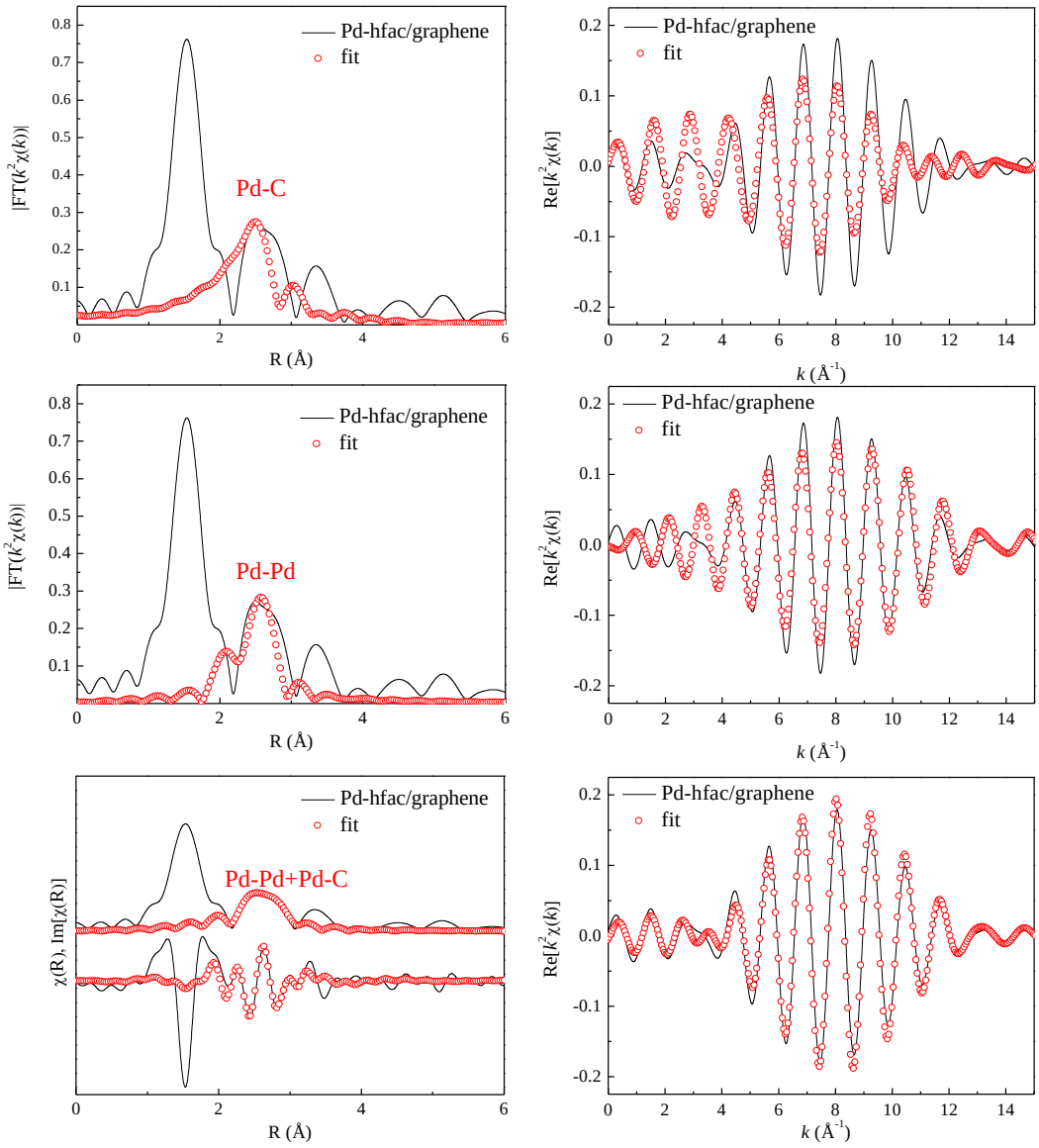

Figure S8. The fitting curve of k^2-weighted EXAFS spectra and $k^2\chi(k)$ oscillations for the second EXAFS FT peak of Pd-hfac/graphene sample. Similar to the fitting for the Pd_1/graphene, it can be found that the curve-fitting of the second EXAFS FT peak by including two shells of Pd-C and Pd-Pd can yield a better quality, compared those cases by considering only Pd-C or Pd-Pd shell. It is worthy to mention that Elam et al. also observed a similar weak peak at ~2.5 Å on the Pd-hfac/TiO_2 sample.[7]

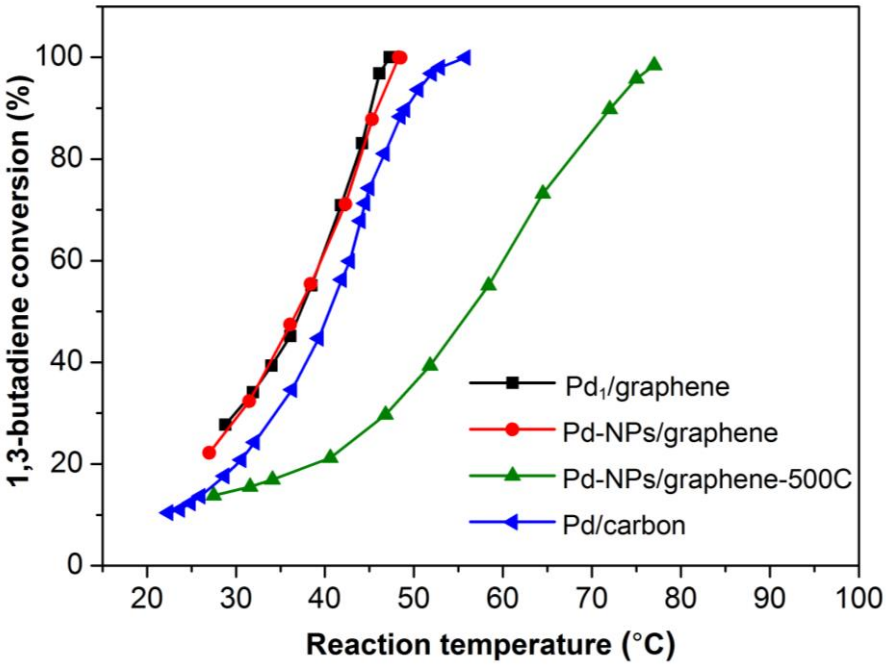

Figure S9. 1,3-butadiene conversion as a function of reaction temperature on the various Pd catalysts.

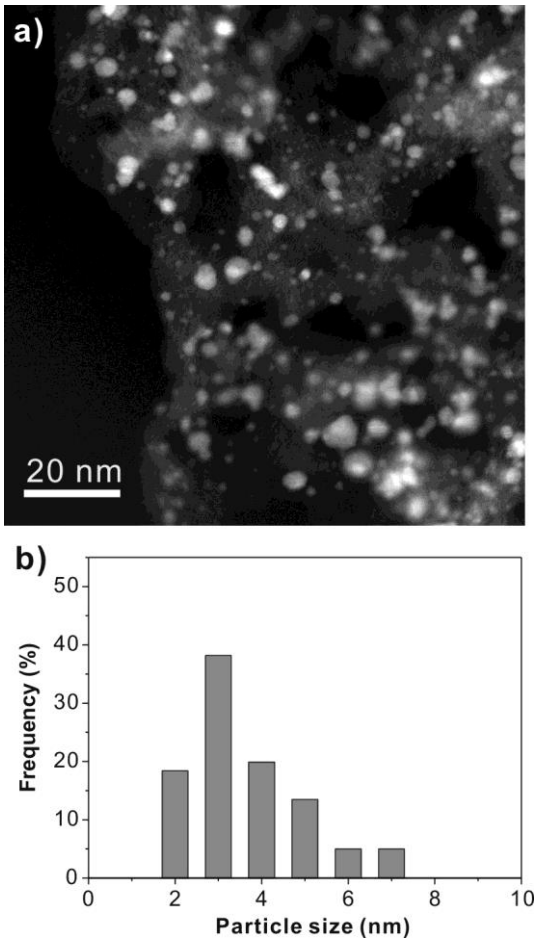

Figure S10. a) A representative aberration-corrected HAADF-STEM image of the commercial Pd/carbon sample (Sigma Aldrich). b) The particle size distribution histogram of Pd nanoparticles on this sample. The average particle size is about 3.6 nm.

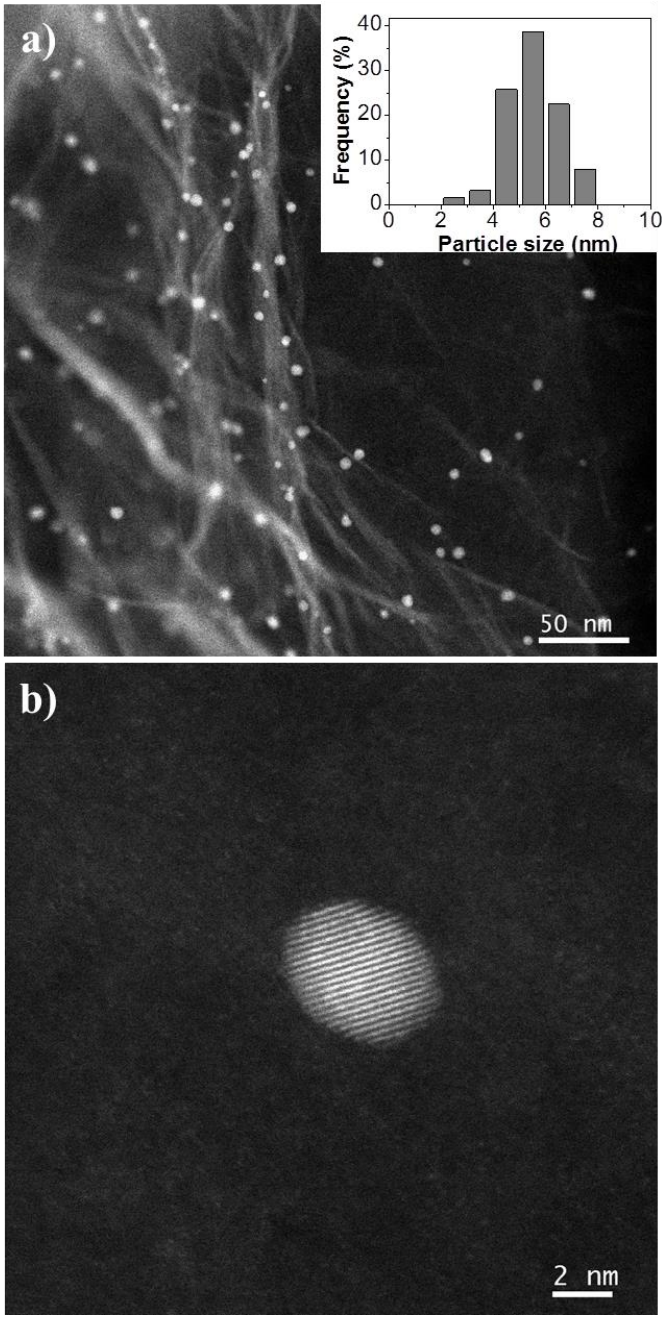

Figure S11. Representative aberration-corrected HAADF-STEM images of Pd-NPs/graphene-500C at low (a) and high (b) magnifications. The insert is the particle size distribution histogram of Pd nanoparticles on this sample. The average particle size is about 5.5 nm.

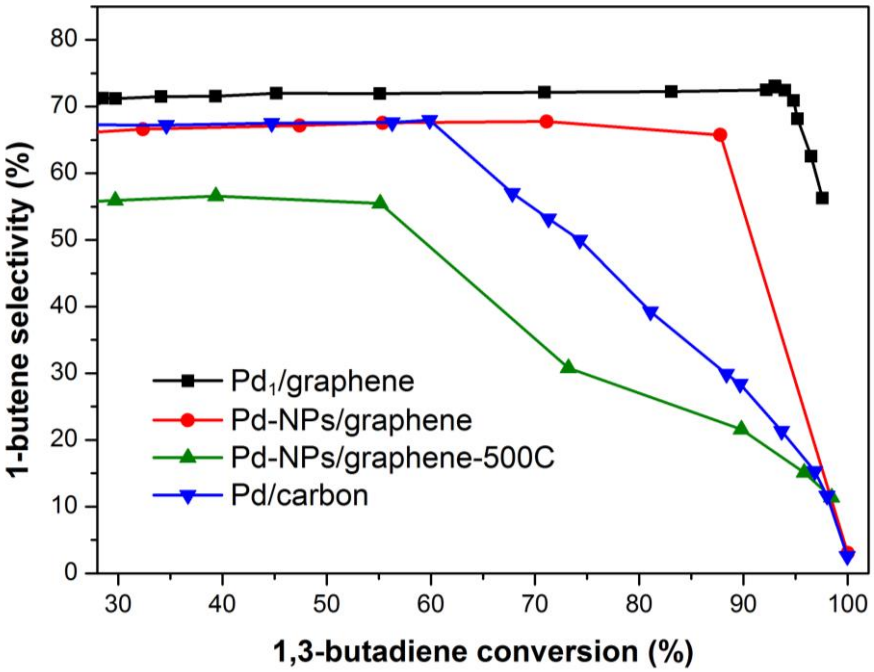

Figure S12. 1-butene selectivity as a function of 1,3-butadiene conversion on Pd_1/graphene, Pd-NPs/graphene, Pd-NPs/graphene-500C, and Pd/carbon samples.

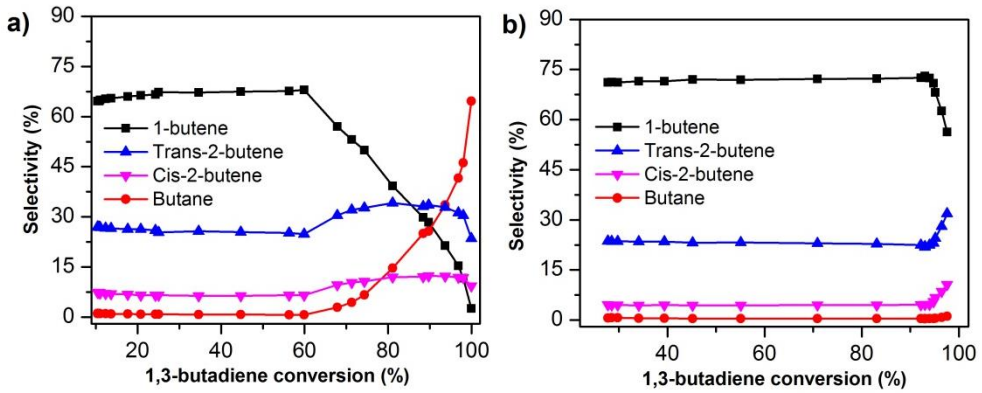

Figure S13 Plots of selectivity as a function of 1,3-butadiene conversion on the Pd/carbon (a) and Pd_1/graphene (b) catalysts in selective hydrogenation of 1,3-butadiene. Pd_1/graphene showed a striking different catalytic performance with Pd/carbon, even though the ranges of reaction temperature are quite close.

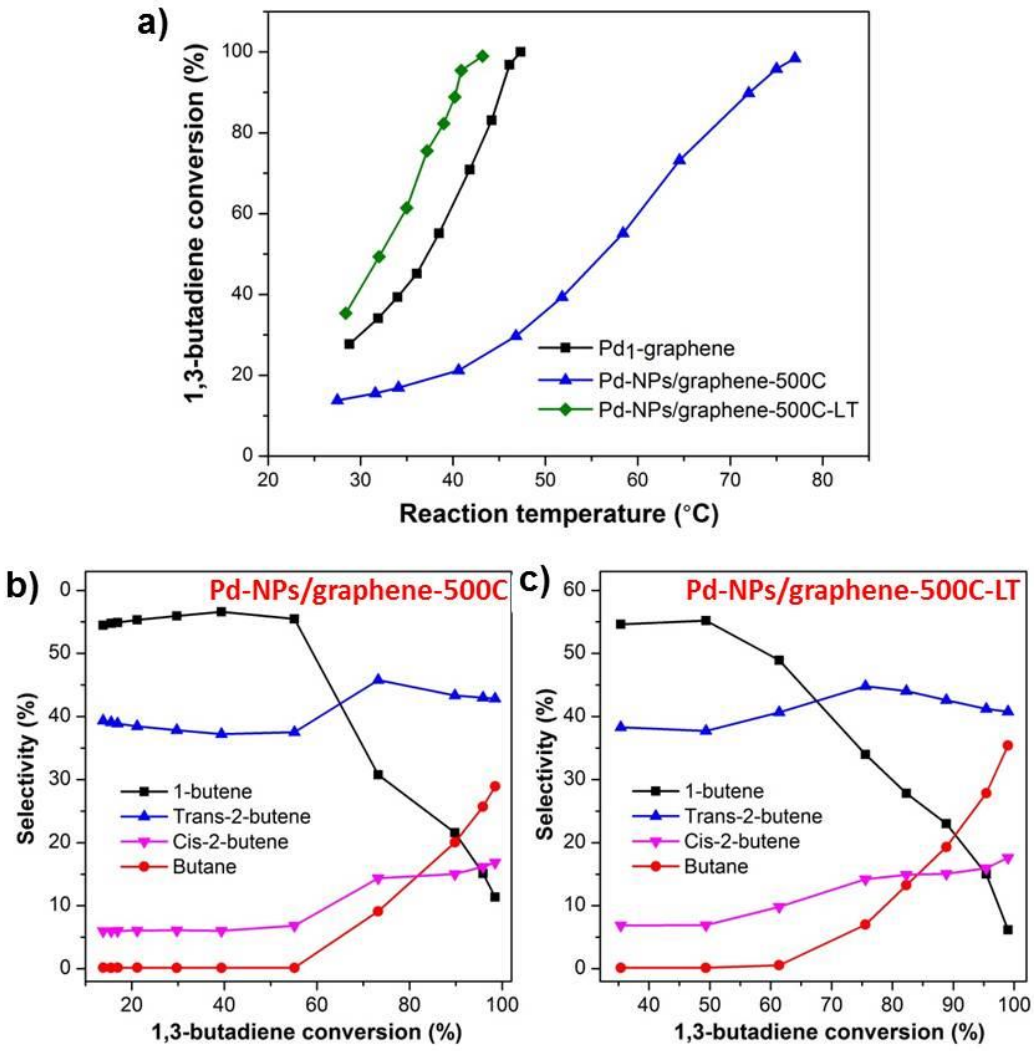

Figure S14 (a) 1,3-butadiene conversion as a function of reaction temperature on the various Pd catalysts. Plots of selectivity as a function of 1,3-butadiene conversion on Pd-NPs/graphene-500C (b) and Pd-NPs/graphene-500C-LT (c) catalysts in selective hydrogenation of 1,3-butadiene.

We further performed the reaction on Pd-NPs/graphene-500C, by increasing the catalyst amount (designated as Pd-NPs/graphene-500C-LT). The temperature for achieving 100% conversion deceased from 78 ^{o}C about 44 ^{o}C, when a larger amount of catalyst were used (Figure S14a). However, no any significant changes in the products selectivity were observed by lowering the reaction temperatures (Figures 14b and c). Moreover, the butenes selectivity on Pd-NPs/graphene-500C-LT was still much lower than Pd_1/graphene at high conversions (Figures S13b and S14c), even though the temperature is lower (Figure S14a).

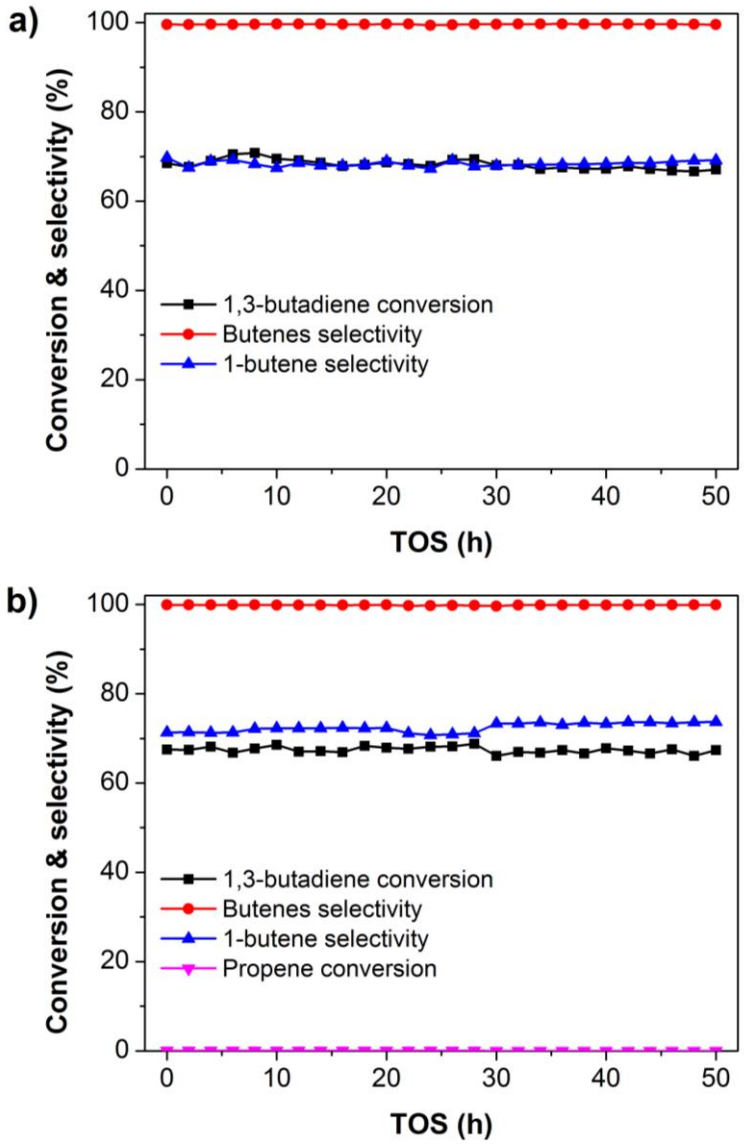

Figure S15. Durability test on the single-atom Pd_1/graphene catalyst first in the absence of propene for 50 h (a), and then in the presence of 70% propene for another 50 h (b) at a 1,3-butadiene conversion of near 70%. TOS = time on stream.

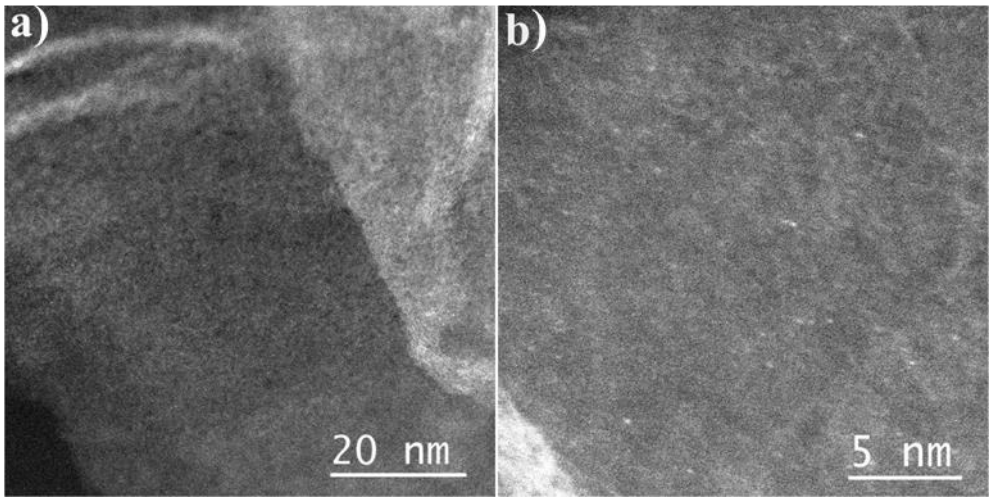

Figure S16. Representative aberration-corrected HAADF-STEM images of single-atom Pd_1/graphene catalyst after a total 100 h of reaction time on stream (TOS) at near 50 ℃.

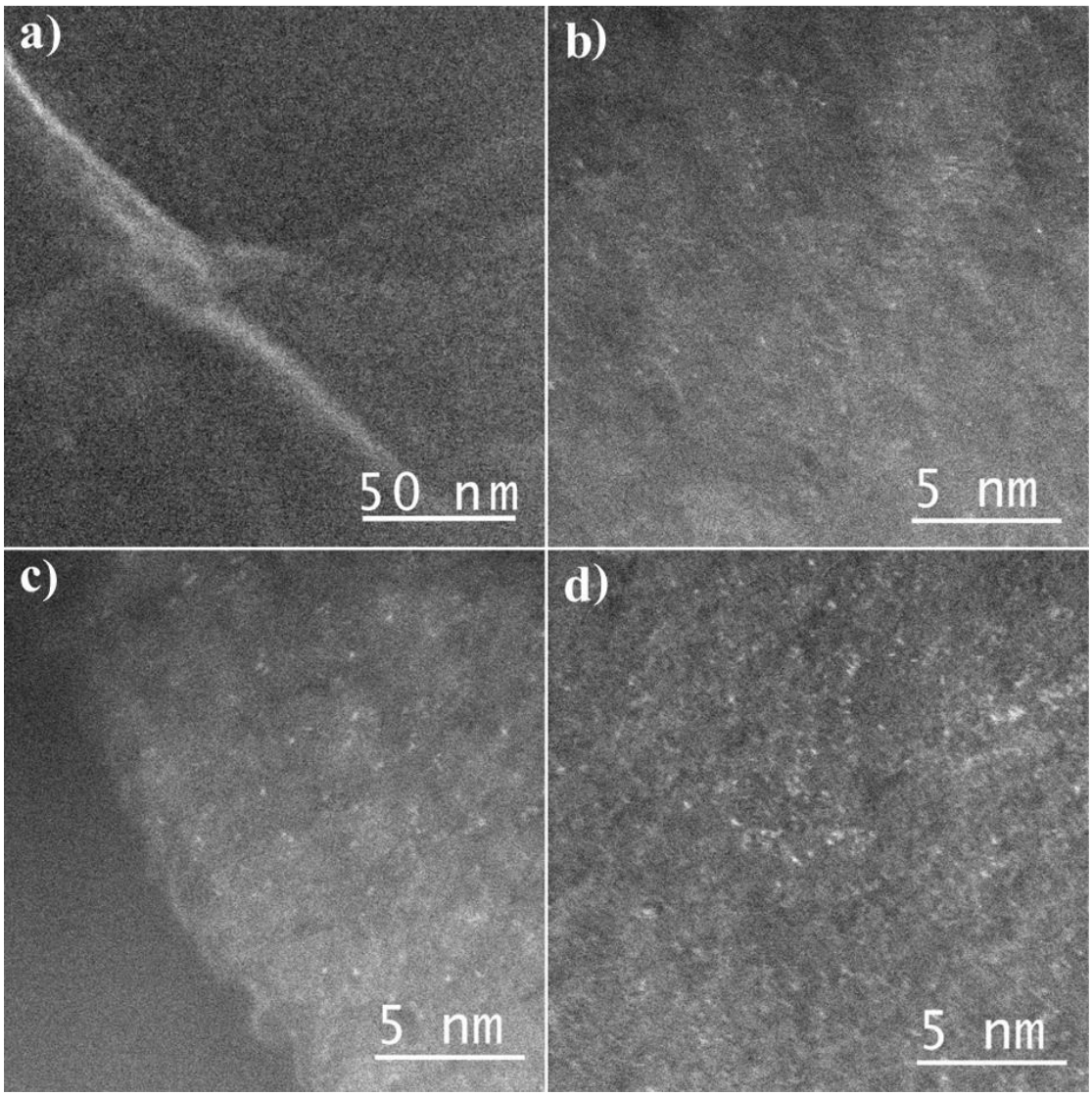

Figure S17. Representative aberration-corrected HAADF-STEM images of single-atom Pd_1/graphene catalyst after annealing at 400 ℃ in Ar at a flow rate of 80 ml/min for 1 h.

Table S1. The Pd loadings on several different graphene supports determined by ICP-AES. These graphene supports were obtained by thermal deoxygenation of graphene oxide at different temperatures for different time under helium at a flow rate of 50 ml/min.

Annealing temperature (℃)	Annealing Time (min)	Pd Loadings (%)
-[a]	-[a]	0.02
700	0.5	1.70
1050	1	1.20
1050	2	0.25
1050	5	0.03
1050	10	0.01

[a] Pristine graphene without any treatment.

Comparing the XPS (Figure S1) results with the Pd loading determined by ICP-AES (Table S1), we revealed that the phenolic oxygen is the nucleation sites for the $Pd(hfac)_2$ precursor, while the C=O (oxygen doubly bound to aromatic carbon denoted as **I1**), C−O (oxygen singly bonded to aliphatic carbon denoted as **I2**) does not seem to react with the $Pd(hfac)_2$ precursor. However, highly dense phenolic oxygen would likely cause the formation of Pd nanoparticles, because considerable fraction of Pd nanoparticles was observed on the graphene support (annealing graphene oxide at 700 ℃ for 0.5 min, Figure S3), wherein XPS showed similar types but larger amount of oxygen species (Figure S1b) .

The atomic percentage of I3 oxygen species apparently higher than the Pd loading on each sample is likely due to that most of the oxygen species are located in the bulk of graphene support.

Table S2. Structural parameters extracted from quantitative EXAFS curve-fitting using the ARTEMIS module of IFEFFIT.[6].

Samples	Path	*N*	*R* (Å)	σ^2 (10^{-3} Å^2)	ΔE_0 (eV)
Pd foil	Pd-Pd	12	2.76	6.5	3.9
PdO	Pd-O	4.0	2.02	3.4	2.0
	Pd-Pd	4.0	3.02	5.2	4.1
$Pd(hfac)_2$	Pd-O	4.0	1.96	2.6	2.1
Pd-NPs/graphene	Pd-Pd	8.7	2.72	8.1	3.8
Pd-hfac/graphene	Pd-C_1[a]	1.0	2.00	3.4	3.9
	Pd-O_1[b]	1.0	2.04	3.7	1.9
	Pd-O_2[b]	2.0	2.08	4.5	2.2
	Pd-Pd	0.3	2.78	7.3	2.1
	Pd-C_2[a]	4.0	2.83	5.4	4.2
Pd_1/graphene	Pd-C_1[a]	1.0	2.00	3.7	4.0
	Pd-O_1[b]	1.0	2.05	3.9	1.9
	Pd-O_2[b]	2.0	2.07	4.9	1.9
	Pd-Pd	0.5	2.78	6.8	1.9
	Pd-C_2[a]	4.0	2.80	5.0	4.2

[a]Carbon atoms C_1 and C_2 provided by the graphene support represents the nearest and the next nearest Pd-C coordinations.

[b]Oxygen atom O_1 bridges Pd atom and the graphene support and Pd-O_2 coordination locates on the side of away from the graphene support.

Table S3. A comparison of catalytic performance in terms of activity and selectivity in selective hydrogenation of 1,3-butadiene. Obviously, the single-atom Pd_1/graphene catalyst demonstrated the highest 1-butene selectivity of 71% at high 1,3-butadiene conversions and low temperatures.

Samples	Pd particle size (nm)	1,3-butadiene to H_2 mole ratio	Reaction Temperature (℃)	Conversion (%)	Butenes selectivity (%)	1-butene selectivity (%)	Notes
Pd_1/graphene	**Single atoms**	**1:2.5**	**47**	**95**	**99.5**	**71**	This work
Pd-NPs/graphene	-[a]	1:2.5	47	94	97	49	This work
Pd-NPs/graphene-500C	5.5	1:2.5	47	30	100	56	This work
Pd/carbon	3.6	1:2.5	47	81	85	39	This work
Pd/Al_2O_3	2.3	1:2.5	47	59	72	39	Ref [4]
Pd/nanofiber	3.4	1:5	50	2	96	40	Ref [8]
Pd/graphite	4	1:5	20	95	5	1.3	Ref [9]
Pd/TiO_2	4.6	1:2	50	3	95	55	Ref [10]
Pd/γ-Al_2O_3	5	1:4	49	10	100	58	Ref [11]
Pd/Al_2O_3	5	1:1.2	25	48	98	46	Ref [12]
Pd/mixed θ/α-Al_2O_3	2	1:1	50	52	98	60	Ref [13]
Pd/α-Al_2O_3	3.1	1:1	50	35	92	55	Ref [13]
Pd/SiO_2	6	1:4	50	4	99	48	Ref [14]
Pd/SiO_2	4.1	1:6.7	40	26	73	38	Ref [22]
Pd/Al_2O_3	3.7	1:6.7	40	37	45	12	Ref [22]
Pd/Si_3N_4	4.3	1:6.7	40	46	56	13	Ref [22]
Pd/SiC	4.5	1:6.7	40	21	57	20	Ref [22]
Pd/TiO_2	4.6	1:2	140	90	95	20	Ref [10]
Pd/γ-Al_2O_3	5	1:2.2	87	60	100	58	Ref [11]

Pd/Al_2O_3 with porous alumina overcoat	2.3	1:2.5	100	95	99.6	56	Ref [4]
$Pd\text{-}Au/Al_2O_3$	-[a]	1:67	120	100	100	40	Ref [15]
Pd-Cu/graphite	1.8	1:5	20	98	10	2.3	Ref [9]
Pd-Sn/mixed $\theta/\alpha\text{-}Al_2O_3$	2	1:1	70	80	100	58	Ref [13]
Pd-Sn/mixed $\theta/\alpha\text{-}Al_2O_3$	2	1:1	50	60	100	58	Ref [13]
$Pd\text{-}Sn/\alpha\text{-}Al_2O_3$	3.2	1:1	50	10	100	56	Ref [13]
$Pd\text{-}Ni/Al_2O_3$	5.9	1:4	72	92	80	30	Ref [14]
$Pd\text{-}Fe/Al_2O_3$	5	1:1.2	25	40	67	52	Ref [12]
Au^{3+}/ZrO_2	Single atoms	1:45	120	85	100	64	Ref [16]
Au/Carbon nanotubes	3.2	1:73	170	100	100	34	Ref [17]
Au/TiO_2	3.5	1:49	183	98	99.7	67	Ref [18]
Au/Al_2O_3	2.5	1:49	185	88	100	65	Ref [18]

[a]Not available.

Table S4. A comparison of catalytic activity in selective hydrogenation of 1,3-butadiene on various catalysts.

Samples	Pd particle size (nm)	1,3-butadiene to H_2 mole ratio	Reaction Temperature (℃)	Conversion (%)	Specific activity per metal atom (s^{-1})	TOF (s^{-1})	Notes
Pd_1/graphene	**Single atoms**	**1:2.5**	**47**	**95**	**0.35**	**0.35**	This work
Pd/carbon	3.6	1:2.5	47	81	0.30	0.96[a]	This work
Pd-NPs/graphene-500C	5.5	1:2.5	47	30	0.11	0.54[a]	This work
Pd-NPs/graphene	-[b]	1:2.5	47	94	0.34	-[b]	This work
Au^{3+}/ZrO_2	Single atoms	1:45	120	85	0.42	0.42	Ref [16]
$Rh(C_2H_4)_2(acac)/MgO$	Mononuclear complexes	1:49	40	27	0.01	0.01	Ref [19]
Cu/TiO_2	1.1	1:100	75	21	9.5×10^{-4}	1.0×10^{-3}	Ref [20]
Au/TiO_2	1.8	1:100	75	10	1.9×10^{-3}	3.4×10^{-3}	Ref [20]
Pd/Al_2O_3	2.3	1:2	47	59	0.18	0.41[a]	Ref [4]
$Pd/\alpha\text{-}Al_2O_3$	2.8	1:5.2	0	-	0.188	0.53	Ref [21]
Pd/Al_2O_3	3.7	1:6.7	40	37	3.2	10.5	Ref [22]
Pd/SiO_2	4.1	1:6.7	40	26	1.8	8.5	Ref [22]
Pd/SiC	4.5	1:6.7	40	20.5	1.6	6.5	Ref [22]
Pd/Si_3N_4	4.3	1:6.7	40	46	4.3	16.5	Ref [22]
$Pd/\alpha\text{-}Al_2O_3$	6	1:5.2	0	-	1.1	6.6	Ref [21]
Pd/C	4	1:49	23	90	0.23	0.92	Ref [23]

[a] Here the dispersion (D%) of Pd nanoparticles was calculated through the following Equation: D = 1.12 /d. Here d is the particle size in nm.[24]

[b] Not available.

Table S5. A comparison of catalytic performance in terms of durability against deactivation in selective hydrogenation of 1,3-butadiene. Again, the single-atom Pd_1/graphene catalyst showed the best ever durability against deactivation, wherein no any visible activity decline was observed during a total 100 h of reaction time on stream.

Samples	Reaction Temperature (℃)	TOS[a] (h)	Initial conversion (%)	Final conversion (%)	Notes
Pd_1/graphene	**52**	**50**	**95[b]**	**95**	**This work**
Pd_1/graphene	**52**	**50**	**~100[c]**	**~100**	**This work**
Pd_1/graphene	**35**	**50**	**70[b]**	**70**	**This work**
Pd_1/graphene	**35**	**50**	**70[c]**	**70**	**This work**
Pd/graphene	20	3	81	45	Ref [9]
Pd/α-Al_2O_3	20	18	22	15	Ref [22]
Pd/Al_2O_3	25	4	90	40	Ref [12]
Pd/SiO_2	20	5	48	3	Ref [22]
Pd/α-Si_3N_4	20	3	35	13	Ref [22]
Pd/β-SiC	20	6	23	9	Ref [22]
Pd-Fe/Al_2O_3	25	5	62	38	Ref [12]
PdAu nanoflowers	35	11	98	98	Ref [25]
Pd black/Pd foil	30	1	100	80	Ref [26]
Pd/Al_2O_3 with porous alumina overcoat	100	62	95[b]	95	Ref [4]
Pd/Al_2O_3 with porous alumina overcoat	100	62	~100[c]	~100	Ref [4]
Au^{3+}/ZrO_2	120	6	90	87	Ref [16]
Au/TiO_2	75	20	10	10	Ref [20]
Cu/TiO_2	75	10	100	26	Ref [20]
Pt/Al_2O_3	25	2	83	27	Ref [12]
Pt-Fe/Al_2O_3	25	4	97	26	Ref [12]

[a]TOS = time on stream. [b]Selective hydrogenation of 1,3-butadiene in the absence of propene. [c]Selective hydrogenation of 1,3-butadiene in the presence of 70% propene.

References.

(1) Hummers, W. S.; Offeman, R. E., *J. Am. Chem. Soc.* **1958**, 80, 1339-1339.

(2) Lu, J.; Stair, P. C., *Langmuir* **2010**, 26, 16486-16495.

(3) Elam, J. W.; Zinovev, A.; Han, C. Y.; Wang, H. H.; Welp, U.; Hryn, J. N.; Pellin, M. J., *Thin Solid Films* **2006**, 515, 1664-1673.

(4) Yi, H.; Du, H. Y.; Hu, Y. L.; Yan, H.; Jiang, H.-L.; Lu, J. L., *ACS Catal.* **2015**, 5, 2735-2739.

(5) Ganguly, A.; Sharma, S.; Papakonstantinou, P.; Hamilton, J., *J. Phys. Chem. C* **2011**, 115, 17009-17019.

(6) Ravel, B.; Newville, M., *J Synchrotron Radiat* **2005**, 12, 537-541.

(7) Lei, Y.; Lu, J. L.; Zhao, H. Y.; Liu, B.; Low, K. B.; Wu, T. P.; Libera, J. A.; Greeley, J. P.; Chupas, P. J.; Miller, J. T.; Elam, J. W., *J. Phys. Chem. C* **2013**, 117, 11141-11148.

(8) Bachiller-Baeza, B.; Pena-Bahamonde, J.; Castillejos-Lopez, E.; Guerrero-Ruiz, A.; Rodriguez-Ramos, I., *Catal. Today* **2015**, 249, 63-71.

(9) Cooper, A.; Bachiller-Baeza, B.; Anderson, J. A.; Rodriguez-Ramos, I.; Guerrero-Ruiz, A., *Catal. Sci. Technol.* **2014**, 4, 1446-1455.

(10) Ortel, E.; Sokolov, S.; Zielke, C.; Lauermann, I.; Selve, S.; Weh, K.; Paul, B.; Polte, J.; Kraehnert, R., *Chem. Mater.* **2012**, 24, 3828-3838.

(11) Hou, R. J.; Ye, W. T.; Porosoff, M. D.; Chen, J. G. G.; Wang, T. F., *J. Catal.* **2014**, 316, 1-10.

(12) Crabb, E. M.; Marshall, R., *Appl. Catal. a-Gen.* **2001**, 217, 41-53.

(13) Pattamakomsan, K.; Ehret, E.; Morfin, F.; Gelin, P.; Jugnet, Y.; Prakash, S.; Bertolini, J. C.; Panpranot, J.; Aires, F. J. C. S., *Catal. Today* **2011**, 164, 28-33.

(14) Hou, R. J.; Porosoff, M. D.; Chen, J. G.; Wang, T. F., *Appl. Catal. A: Gen.* **2015**, 490, 17-23.

(15) Hugon, A.; Delannoy, L.; Krafft, J. M.; Louis, C., *J. Phys. Chem. C* **2010**, 114, 10823-10835.

(16) Zhang, X.; Shi, H.; Xu, B. Q., *Angew. Chem. Int. Ed.* **2005**, 44, 7132-7135.

(17) Zhang, X.; Guo, Y. C.; Zhang, Z. C.; Gao, J. S.; Xu, C. M., *J. Catal.* **2012**, 292, 213-226.

(18) Okumura, M.; Akita, T.; Haruta, M., *Catal. Today* **2002**, 74, 265-269.

(19) Yardimci, D.; Serna, P.; Gates, B. C., *ACS Catal.* **2012**, 2, 2100-2113.

(20) Delannoy, L.; Thrimurthulu, G.; Reddy, P. S.; Me´thivier, C.; Nelayah, J.; Reddy, B. M.; Ricolleaud, C.; Louisab, C., *Phys. Chem. Chem. Phys.* **2014**, 16, 26514--26527.

(21) Goetz, J.; Volpe, M. A.; Touroude, R., *J. Catal.* **1996**, 164, 369-377.

(22) Cervantes, G. G.; Aires, F. J. C. S.; Bertolini, J. C., *J. Catal.* **2003**, 214, 26-32.

(23) Zhang, Z. C.; Zhang, X.; Yu, Q. Y.; Liu, Z. C.; Xu, C. M.; Gao, J. S.; Zhuang, J.; Wang, X., *Chem-Eur J* **2012**, 18, 2639-2645.

(24) Lear, T.; Marshall, R.; Lopez-Sanchez, J. A.; Jackson, S. D.; Klapotke, T. M.; Baumer, M.; Rupprechter, G.; Freund, H. J.; Lennon, D., *J. Chem. Phys.* **2005**, 123, 174706.

(25) Chen, H. M.; Huang, J. L.; Huang, D. P.; Sun, D. H.; Shao, M. H.; Li, Q. B., *J Mater Chem A* **2015**, 3, 4846-4854.

(26) Gaube, J.; Klein, H. F., *Appl. Catal. a-Gen.* **2014**, 470, 361-368.